applied sciences

MDPI

Article

Study on Abnormal Pattern Detection Method for In-Service Bridge Based on Lasso Regression

Huaqiang Zhong [1], Hao Hu [1], Ning Hou [2,*] and Ziyuan Fan [2]

[1] Zhejiang Engineering Center of Road and Bridge Intelligent Operation and Maintenance Technology, Hangzhou 310018, China; zhonghuaqiang0524@163.com (H.Z.); hhu@zjjtkyy.com (H.H.)
[2] School of Civil Engineering and Architecture, Zhejiang Sci-Tech University, Hangzhou 310018, China; fanzy1216@163.com
* Correspondence: houning@zstu.edu.cn

Abstract: The real-time operational safety of in-service bridges has received wide attention in recent years. By fully utilizing the health monitoring data of bridges, a structural abnormal pattern detection method based on data mining can be established to effectively ensure the safety of in-service bridges. This paper takes a large-span arch bridge as the research object, analyzes the time-based variation of the main monitoring data of the structure, establishes Lasso regression models for load characteristic indicators and vertical bending fundamental frequency of the structure under different time scales, and uses the residuals of the Lasso model to indicate the structural state and identify abnormal patterns. Firstly, the monitoring data of bridge structural temperature, girder end displacement, and girder acceleration were analyzed, and the interrelationships were studied to extract characteristic parameters of structural load characteristics and structural frequency. Then, the time-varying patterns of structural response were analyzed, and Lasso regression models and their regression variables were discussed based on monitoring data under two different time scales: daily cycle and annual cycle. The abnormal pattern detection method for bridge structures was developed. Finally, the effectiveness of this method was verified by taking the bridge deck pavement replacement as the abnormal pattern. The research results indicate that the proposed bridge structure abnormal pattern detection method based on Lasso regression can effectively monitor changes in the state of the bridge, and the residual dispersion of the model established on the annual cycle scale is relatively smaller than that on the daily cycle scale, resulting in better abnormal detection performance.

Keywords: bridge engineering; structural health monitoring; Lasso regression; data analysis; abnormal pattern detection; deck pavement

check for updates

Citation: Zhong, H.; Hu, H.; Hou, N.; Fan, Z. Study on Abnormal Pattern Detection Method for In-Service Bridge Based on Lasso Regression. *Appl. Sci.* **2024**, *14*, 2829. https://doi.org/10.3390/app14072829

Received: 1 February 2024
Revised: 25 March 2024
Accepted: 26 March 2024
Published: 27 March 2024

Copyright: © 2024 by the authors. Licensee MDPI, Basel, Switzerland. This article is an open access article distributed under the terms and conditions of the Creative Commons Attribution (CC BY) license (https://creativecommons.org/licenses/by/4.0/).

1. Introduction

In China, there is a massive number of bridges, and many of the large-span bridges serve as core nodes in the road network, holding significant importance for economic development. To ensure the structural safety of these large-span bridges, many important bridges have been equipped with structural health monitoring (SHM) systems of varying complexity [1,2]. However, currently, the immense data collected by these SHM systems are not fully utilized, and the goals of achieving real-time monitoring of structural conditions and detection of abnormal patterns still remain challenging tasks [3,4].

One of the primary objectives of structural health monitoring of bridges is to achieve real-time monitoring of the structural condition by conducting in-depth analysis of the data collected through sensors and subsequently identifying abnormal patterns such as structural damage [5,6]. Since the last century, numerous studies have been carried out on abnormal pattern detection methods based on structural monitoring data [3,7,8]. In these studies, the indexes used to identify anomalous modes included frequency, vibration pattern, and modal strain energy, among others [9–11]. However, the validity of these

indexes has only been proven in easily controlled environments like numerical simulation or laboratory experiments, and their application to in-service bridges is limited. As research progresses, there is increasing focus on analyzing the long-term evolution pattern of structural monitoring data and the correlation among the data. This data-driven approach aims to extract the mapping relationship between inputs and outputs, thus providing a basis for assessing the structural condition [12].

Most of the data-driven research on the static characteristics of structures starts from the perspective of the correlation between load and static response and aims to construct indicators that are insensitive to structural conditions. Li et al. constructed a feature quantity that is only related to the lateral position of vehicles by using the ratio of the cable tension upstream and downstream of a bridge, which enables the identification of cable breakage [13]. Yang et al. conducted a study on the identification of cable tension based on the vibration amplitude of cable-stayed bridges and suggested using time intervals with relatively small amplitude and stable vibration for cable tension identification [14]. Tian et al. used a BiLSTM model to establish the mapping relationship between the deflection of the main girder and cable tension and employed the deflection information to identify abnormal cable tension [15]. In addition, there is a high linear correlation between the longitudinal deformation of the main girder and temperature, with the main beam showing a tendency to elongate with increasing temperature [16]. This characteristic can be utilized for structural abnormality detection.

The research progress in the field of structural dynamic characteristics is not significant. This is because the on-site environment of the structure changes, and its dynamic characteristics also vary over time. At the same time, wind action, traffic load, and temperature action, as the main influencing factors, also vary over time [17–19]. Therefore, the detection of abnormal structural dynamic characteristics needs to firstly eliminate the normal variation component caused by variable action. Hang et al. proposed an abnormality detection method that integrates kernel canonical correlation analysis and cointegration theory to deal with the nonlinearity of monitoring data in practical engineering [20]. Wang et al. used a method based on the Bayesian framework to achieve data component separation and structural state identification [21]. Zhou et al. analyzed the quantitative and transfer relationships between on-site environment and bridge modal frequency, reduced the variability of bridge modal frequency, and highlighted the frequency changes caused by an abnormal structural state [22]. Lu et al. achieved integrated signal decomposition and modal parameter identification using improved EMD and COV-SSI methods [23].

In recent years, machine learning methods have been heavily utilized for structural abnormal pattern recognition. These methods mainly include sparse Bayesian learning methods and deep convolutional neural network methods. Hou et al. utilized sparse Bayesian learning methods to improve the robustness of structural damage recognition [24]. Xie et al. introduced the Laplace prior probability model into sparse Bayesian learning, obtaining a more efficient computational model for structural damage recognition and reducing the model's limitation relating to the dataset [25]. Oh et al. defined the residual as the structural damage indicator by comparing the predicted output of the convolutional neural network with the true response in the healthy state of the structure [26]. Ren et al. proposed a method combining Kriging and Artificial Neural Networks to build an evaluation model and improve its prediction accuracy [27]. However, the current methods for identifying abnormal states in structural dynamic characteristics all have their own limitations, and many of the applications for identifying anomalies in structural dynamic characteristics have not been tested in practical bridges. Further research is still needed in this area.

In order to ensure the structural safety of in-service bridges, this paper conducts research on a structure abnormal pattern detection method based on real-time health monitoring data analysis. Taking a large-span arch bridge as the research object, the paper analyzes the temporal variation patterns and correlation relationships of the monitoring data, extracts characteristic indicators, and establishes Lasso regression models and their

regression variables considering the characteristics of the monitoring data under different time scales. Based on the regression residuals, a bridge structure abnormal pattern detection method is proposed, and verification analysis is conducted in combination with practical cases.

2. Description of Arch Bridge and Monitoring Data

This paper takes a large-span arch bridge as the research object. The span arrangement of this large-span arch bridge is $(100 + 450 + 100)$ m, with a slenderness ratio of $1/5$ and a total width of 45.8 m. The structural form is a center-supported steel beam composite system, with the side span arch ribs and the middle span arch ribs in the same plane, and a lateral inclination ratio of 1:5. The arch ribs are connected by transverse braces and K-braces to form a strong lateral bending rigidity to resist the wind load in the transverse direction of the bridge. The stiffening girders are supported on the arch ribs by suspender rods or pillars, and the two ends of the middle span stiffening beam are supported on the transverse girder at the intersection of the middle span arch ribs. The end supports are longitudinal sliding supports with transverse limit supports and longitudinal dampers. The side span stiffening girders are fixed to the arch ribs at the intersection of the middle span and the side span. Powerful horizontal tension members are arranged between the transverse girders at the ends of the main bridge to balance the horizontal thrust of the middle span arch ribs.

Due to its importance as a major cross-river road, the bridge carries a huge traffic volume and suffers from serious overload. In order to continuously monitor the on-site environment and structural status of the bridge, a comprehensive SHM system has been installed; the main sensor layout is shown in Figure 1. Among the sensors, A1∼A15 are accelerometer sensors, T1∼T28 are temperature sensors, and D1∼D4 are beam displacement sensors.

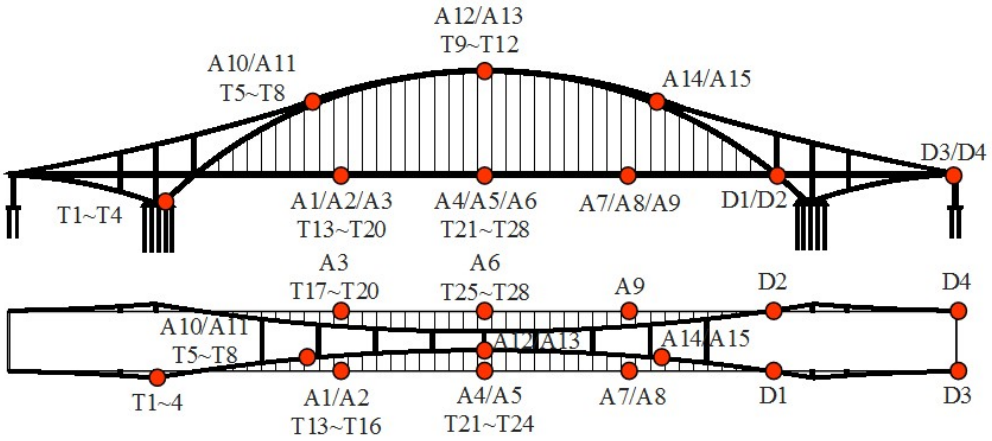

Figure 1. Layout of the sensors.

3. Lasso Regression Theory

When there is only one main influencing factor (independent variable) for the outcome (dependent variable), the variation can be explained using the theory of simple linear regression. However, in research on real-world problems, the variation of the dependent variable is often influenced by several important factors (independent variables). In such cases, it is necessary to use two or more influencing factors as independent variables to explain the changes in the dependent variable. This is known as multiple regression. When there is a linear relationship between multiple independent variables and the dependent variable, the regression analysis conducted is called multiple linear regression. Assuming that a dependent variable y_i is influenced by k independent variables, $x_1, x_2, \ldots, x_k$, the basic equation of a multiple linear regression model is:

$$y_i = \omega_0 + \sum_{j=1}^{k} x_{ij}\omega_j \tag{1}$$

where ω_j is the partial regression coefficient, ω_0 is the intercept, and k is the number of independent variables. The values of ω_j and ω_0 can be obtained using the ordinary least-squares method (LSM) by setting the partial derivative of the objective function in Equation (2) to zero. The objective function is defined as the sum of squared residuals, which is the difference between the true response and the predicted response.

$$argmin \sum_{i=1}^{N} (y_i - \omega_0 - \sum_{j=1}^{k} x_{ij}\omega_j)^2 \tag{2}$$

where N represents the total number of samples.

To enhance the nonlinear fitting capability of the regression model, it is common to add higher-order terms of the initial variables X and then transform it into a linear regression problem for solving. However, this approach poses issues; artificially selecting the number of input variables and increasing the feature dimensionality can result in multicollinearity among variables and the introduction of non-important variables. Therefore, it can lead to overfitting and excessive variance in parameter estimation when directly using ordinary LSM to compute the parameters ω_j and ω_0.

This paper uses Lasso (Least Absolute Shrinkage and Selection Operator) regression to solve the problems of overfitting and excessive parameter estimation variance [28]. Lasso regression is a sparse statistical learning method that adds a penalty term (regularization term) L_1 to the objective function of conventional least-squares solving, as shown in Equation (3). Its Lagrange equivalent form is shown in Equation (4).

$$argmin\{\frac{1}{2N} \sum_{i=1}^{N} (y_i - \omega_0 - \sum_{j=1}^{k} x_{ij}\omega_j)^2\}, s.t. \sum |\omega_j| \leq t \tag{3}$$

$$argmin\{\frac{1}{2N} \sum_{i=1}^{N} (y_i - \omega_0 - \sum_{j=1}^{k} x_{ij}\omega_j)^2 + \lambda \sum_{j=1}^{k} |\omega_j|\} \tag{4}$$

where t and λ are both regularization coefficients, and they have a one-to-one correspondence. The sizes of t and λ determine the complexity of the Lasso regression model. Generally speaking, the larger the value of t (smaller λ), the more complex the Lasso regression model; conversely, the smaller the value of t (larger λ), the simpler the Lasso regression model. A simpler Lasso model implies that the model requires sparser feature coefficients as input. A larger λ can easily lead to overfitting of the regression model, while a smaller λ can easily lead to underfitting. Therefore, it is necessary to determine an appropriate value of λ to establish a suitable Lasso regression model [29].

Since λ is a hyperparameter, it cannot be obtained during the training of the regression model and needs to be manually specified. However, λ has a significant impact on the performance of the Lasso regression model, and it is crucial to select the optimal value when building the Lasso regression model. This paper uses cross-validation techniques to determine the value of λ. Taking k-fold cross-validation as an example, the dataset is divided into k groups, with one group serving as the validation set and the remaining $(k-1)$ groups as the training set. Different values of λ are used to train the Lasso regression model on the training set, and the predictive ability of the model is evaluated using the validation set. This process is repeated k times to obtain the mean squared error for a specific λ, as shown in Equation (5).

$$MSE_j = \frac{1}{h} \sum_{i=1}^{h} (y_i - \hat{y}_i)^2 \tag{5}$$

where $h = N/k$, and $\hat{y}_i$ represents the estimated value of the response y_i.

The mean squared error (MSE) of the cross-validation can be obtained by taking the average of the MSEs of the k-fold cross-validation, as shown in Equation (6).

$$CV(p) = \frac{1}{k}\sum_{i=1}^{k} MSE_j \tag{6}$$

In theory, the optimal value of λ for establishing the Lasso regression model can be chosen as the value corresponding to the minimum mean-squared error of the cross-validation. However, it is also necessary to consider the complexity of the regression model and the prediction accuracy based on the specific problem. It is generally recommended to select the λ value corresponding to the minimum mean squared error plus one standard deviation as the final parameter. This is because, as λ increases, the regression coefficients become sparser. Without significantly increasing the prediction error, it is preferable to choose larger λ values.

4. Monitoring Data Analysis

4.1. Temperature Effect Analysis

Based on the monitoring data from the SHM system of this bridge, this paper compared the temperatures of various components of the girder and arch rib over two consecutive days in different seasons, as illustrated in Figure 2. Specifically, Figure 2a depicts the temperature variations of the bridge during summer, whereas Figure 2b illustrates the temperature fluctuations during winter. From the figures, it can be seen that the temperature distribution of the girder and arch rib is relatively uniform under the influence of solar radiation. This is because the bridge is made of steel, which has fast heat conduction. Among the six temperature measurement points under direct sunlight, except for the temperature of the right side of the girder's top plate and the right side of the arch rib, the overall temperature variation of the measurement points is basically synchronized, and there is a significant temperature difference between day and night.

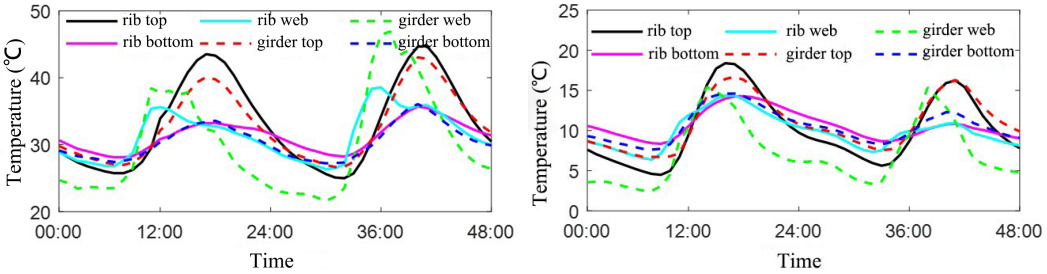

Figure 2. Temperature monitoring data. (**a**) Heating. (**b**) Cooling.

4.2. Structural Acceleration and Gross Vehicle Weight Data Analysis

Considering the poor continuous operation characteristics of the weigh-in-motion (WIM) system, this paper uses the root mean square (RMS) of the measured structural acceleration as the equivalent traffic load to ensure the quality of data analysis. The scatter plot of the structural acceleration RMS and the WIM data is shown in Figure 3. From the figure, it can be seen that there is a correlation between the gross vehicle weight (GVW) and the structural acceleration RMS. In particular, Figure 3b shows a more obvious correlation compared to Figure 3a because Figure 3b does not include GVWs of less than 5 tons. Although there are many small vehicles with GVWs of less than 5 tons, and they account for a large proportion of the total number of vehicles, their influence on the structural frequency is small, and their contribution to the structural acceleration RMS is not significant, so they can be removed from the analysis process. The above analysis indicates that using the acceleration RMS as the equivalent traffic load is feasible.

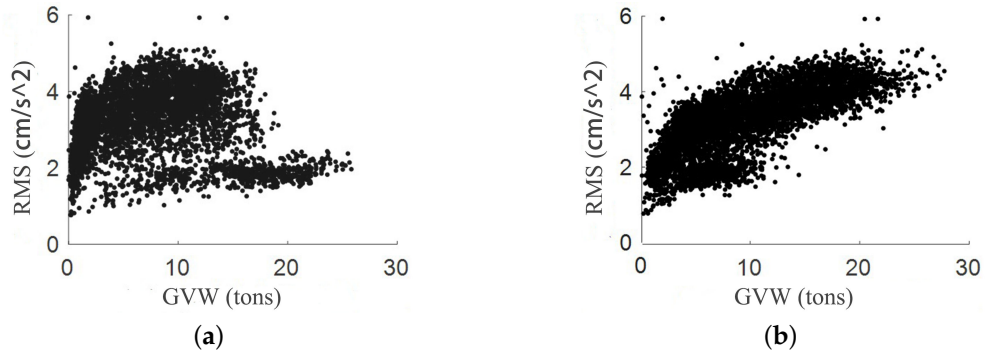

Figure 3. Scatter plot of acceleration by RMS and GVW. (**a**) All GVWs. (**b**) GVWs of more than 5 tons.

4.3. Longitudinal Displacement Analysis

This paper presents a statistical analysis of the longitudinal displacement data of the girder along with the temperature data of the girder bottom plate. The results are shown in Figure 4. From the figure, it can be seen that there is a strong linear correlation between the longitudinal displacement of the side span girder (at DT3 and DT4) and the temperature of the girder bottom plate. However, the linear correlation between the longitudinal displacement of the middle span girder (at DT1 and DT2) and the temperature of the girder bottom plate shows an increased level of dispersion. This is because the side span girder of the structure, under the action of tension rods, experiences a force state similar to that of a cable-stayed bridge, while the middle span girder experiences a force state similar to that of a suspension bridge. Therefore, the middle span girder undergoes longitudinal oscillations under the influence of vehicle loads, which increases the dispersion in the results of the correlation analysis. This also indicates that the longitudinal displacement of the girder is not only related to the thermal expansion and contraction of the bridge components but also to the force state of the components.

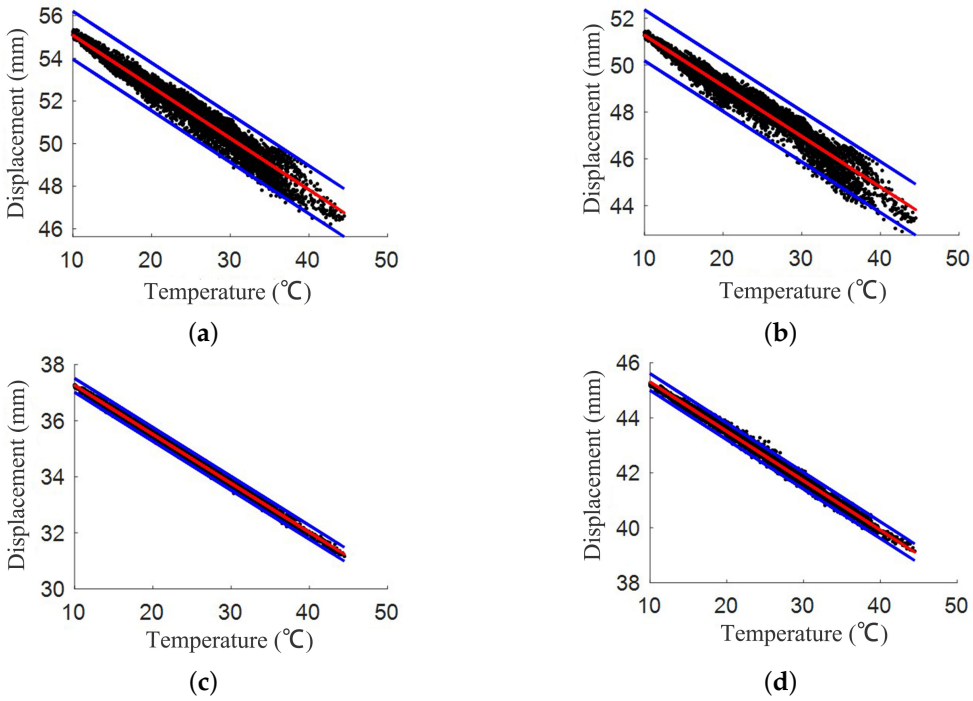

Figure 4. Scatter plot of girder displacement and girder bottom plate temperature. (**a**) Girder displacement at DT1. (**b**) Girder displacement at DT2. (**c**) Girder displacement at DT3. (**d**) Girder displacement at DT4.

4.4. Structural Frequency Analysis

During the service of bridge structures, they are significantly influenced by the on-site environment, and their dynamic characteristics also change over time. In this paper, the NexT + ERA algorithm is used to identify the vertical bending frequency. The results are shown in Figure 5, where the second-order vertical bending frequency represents the structural vertical fundamental frequency.

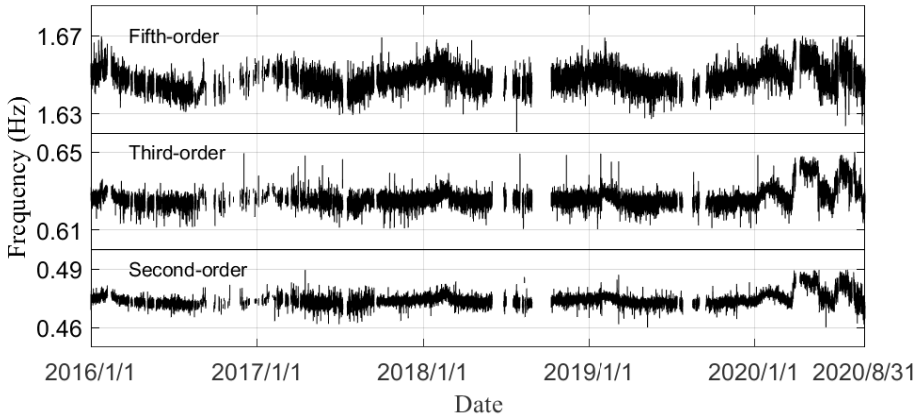

Figure 5. Structural frequency.

From Figure 5, it can be seen that the structural frequency varies due to the effects of the on-site environment, loading conditions, and structural performance. The interaction between piles and soil significantly influences the structural frequency [30]. However, this paper fails to address the impact of pile–soil interaction on the structural frequency because the main focus of this paper is the changes in structural frequency. Furthermore, the magnitude of the changes in different-order frequencies over time is not the same. It is difficult to determine the structural state in practical engineering by using a fixed threshold.

5. Lasso Regression Model Based on Monitoring Data

Based on the analysis of the SHM data, this paper further explores the correlations between various types of data. Specifically, the power spectral density (PSD) of equivalent traffic load, structural temperature, and structural vertical fundamental frequency were analyzed separately. The results are shown in Figure 6. In this paper, the horizontal axis of the PSD has been adjusted from frequency to period (the inverse of frequency) to emphasize the impact of long-period components at lower frequencies. From the figure, it can be observed that there are two different periodic components present in the equivalent traffic load, structural temperature, and structural vertical fundamental frequency, namely, 24 h and 8192 h. These two periods correspond to different time scales: 1 day and 1 year, respectively. Therefore, based on these two different time scales, a quantitative model for the relationship between load and structural vertical fundamental frequency is established in this paper.

According to the basic theory of Lasso regression algorithm and bridge monitoring data, this paper establishes two different time scales for the Lasso regression models: daily cycle and annual cycle. The input variables for the Lasso regression model of structural temperature are shown in Table 1. The input variables for the Lasso regression model of equivalent traffic load are shown in Table 2.

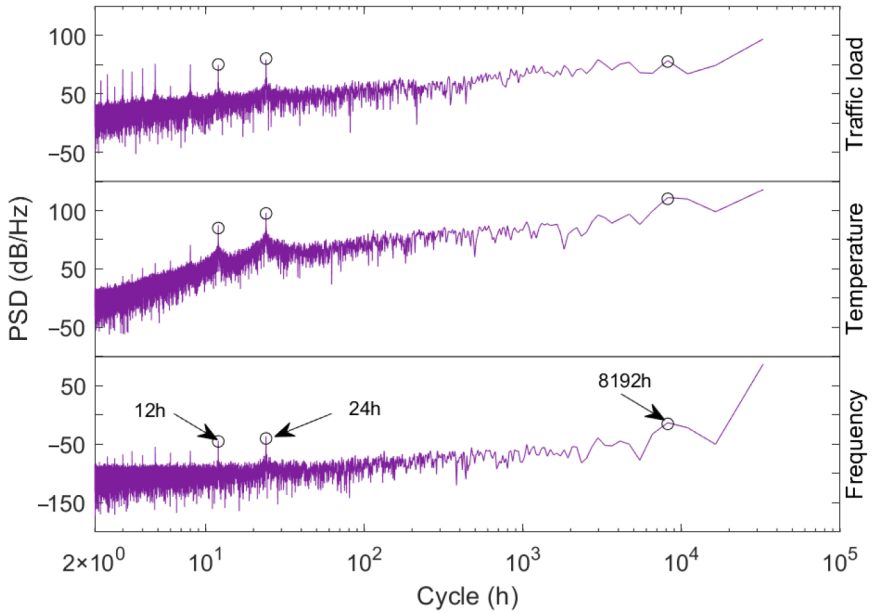

Figure 6. Power spectral density of structural response and fundamental frequency.

Table 1. The structural temperature variables of the Lasso regression model under different time scales.

Time Scale	Structural Temperature Variables	Explanation
Daily cycle	$x_{i-a}^{tpc-d}, x_{m-b}^{t-d}$ $(i = 1 \sim 6, m = 1 \sim 8)$ $(a = 0 \sim 12, b = 0 \sim 12)$	x_i^{tpc-d} represents the first-order term of the principal component; x_m^{t-d} represents the first-order term of the m-th temperature measurement point. a and b represent frequency lag time (unit: hours). In other words, x_{i-a}^{tpc-d} is shifted an hour later than x_{i-0}^{tpc-d}.
Daily cycle	$x_{ij-a}^{tpc-d}, x_{mn-b}^{t-d}$ $(i = 1 \sim 6, j = 1 \sim 6)$ $(m = 1 \sim 8, n = m \sim 8)$	x_{ij}^{tpc-d} represents the second-order term of the principal component; x_{mn}^{t-d} represents the second-order term of the m-th temperature measurement point.
Daily cycle	$x_{ijk-a}^{tpc-d}, x_{mns-b}^{t-d}$ $(i = 1 \sim 6, j = 1 \sim 6)$ $(k = j \sim 6, m = 1 \sim 8)$ $(n = m \sim 8, s = n \sim 8)$	x_{ijk}^{tpc-d} represents the third-order term of the principal component; x_{mns}^{t-d} represents the third-order term of the m-th temperature measurement point.
Annual cycle	x_1^{tpc-y}	x_1^{tpc-y} represents the first-order term of the principal component of the annual cyclic temperature variables.
Annual cycle	x_{11}^{tpc-y}	x_{11}^{tpc-y} represents the second-order term of the principal component of the annual cyclic temperature variables.
Annual cycle	x_{111}^{tpc-y}	x_{111}^{tpc-y} represents the third-order term of the principal component of the annual cyclic temperature variables.

Table 2. The equivalent traffic load of the Lasso regression model under different time scales.

Time Scale	Equivalent Traffic Load	Explanation
Daily cycle	x_i^{a-d} $(i = 1 \sim 3)$	x_i^{a-d} represents the first-order term of the RMS of the acceleration.
Daily cycle	x_{ij}^{a-d} $(i = 1 \sim 3, j = i \sim 3)$	x_{ij}^{a-d} represents the second-order term of the RMS of the acceleration.
Daily cycle	x_{ijk}^{a-d} $(i = 1 \sim 3, j = i \sim 3, k = j \sim 3)$	x_{ijk}^{a-y} represents the third-order term of the RMS of the acceleration.
Annual cycle	x_i^{a-y} $(i = 1 \sim 3)$	x_i^{a-d} represents the first-order term of the RMS of the acceleration under annual cycle.
Annual cycle	x_{ij}^{a-y} $(i = 1 \sim 3, j = i \sim 3)$	x_{ij}^{a-y} represents the second-order term of the RMS of the acceleration under annual cycle.
Annual cycle	x_{ijk}^{a-y} $(i = 1 \sim 3, j = i \sim 3, k = j \sim 3)$	x_{ijk}^{a-y} represents the third-order term of the RMS of the acceleration under annual cycle.

Based on the aforementioned methods for solving the Lasso model parameters, this paper employs cross-validation techniques to calculate the MSE and standard deviation of the Lasso regression model at different λ values. Taking into account the complexity and fitting accuracy of the Lasso regression model, the values of λ for the daily and annual scales of the Lasso regression model are determined separately, as shown in Figure 7. Once the values of λ are determined, the Lasso regression models can be established based on the SHM data.

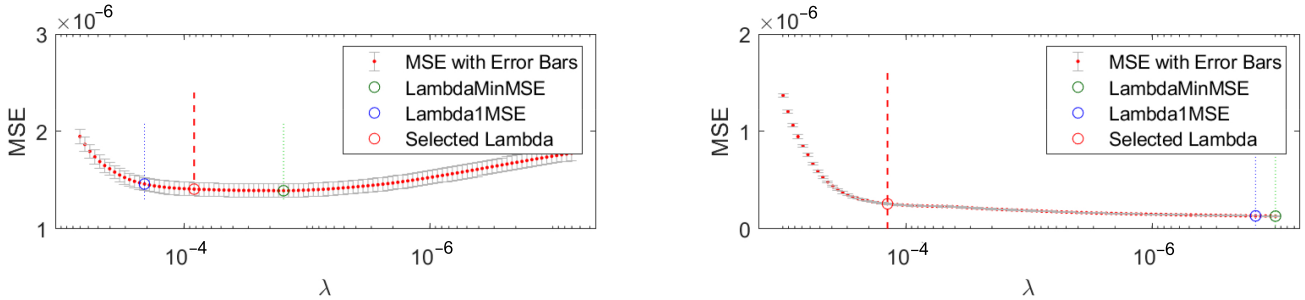

Figure 7. Cross-validated MSE of Lasso fit. (**a**) Daily cycle. (**b**) Annual cycle.

In order to further improve the prediction accuracy of the Lasso regression model, this paper utilizes machine learning methods based on the monitoring data of the bridge to train and validate the model. Specifically, the monitoring data from 17 March 2016 to 31 December 2018 are selected as the training set, and the monitoring data from 1 January 2019 to 31 December 2019 are selected as the test set. The Lasso regression models trained by machine learning are used to predict the residuals in the test set at different time scales, as shown in Figure 8. From the figure, it can be observed that the Lasso regression model under the annual cycle scale has less prediction dispersion, while the Lasso regression model under the daily cycle scale has more prediction dispersion. In other words, as the time scale decreases, the prediction results of the Lasso regression model are more influenced by random factors, and the degree of residual dispersion also increases significantly.

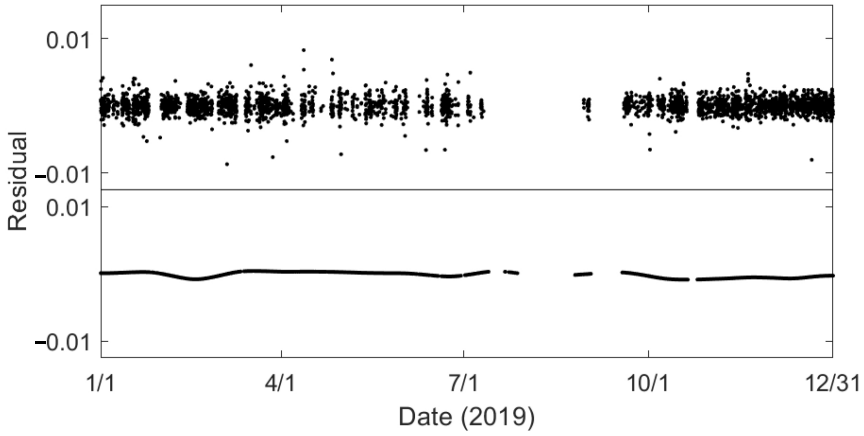

Figure 8. Predictive residual on test set.

The paper also compares the total residuals obtained from Lasso regression analysis of the vertical fundamental frequency with the distribution characteristics of the original data in order to evaluate the distribution condition of the data after regression and analyze the differences between the two. The results are shown in Figure 9. As can be seen from the figure, after regression analysis, the normal variation components of the structural frequency caused by load and environmental effects are eliminated. The distribution width of the frequency prediction residuals is narrower compared to the original data, and its standard deviation is reduced by more than 25% compared to the original data, which is more conducive to judging the structural condition.

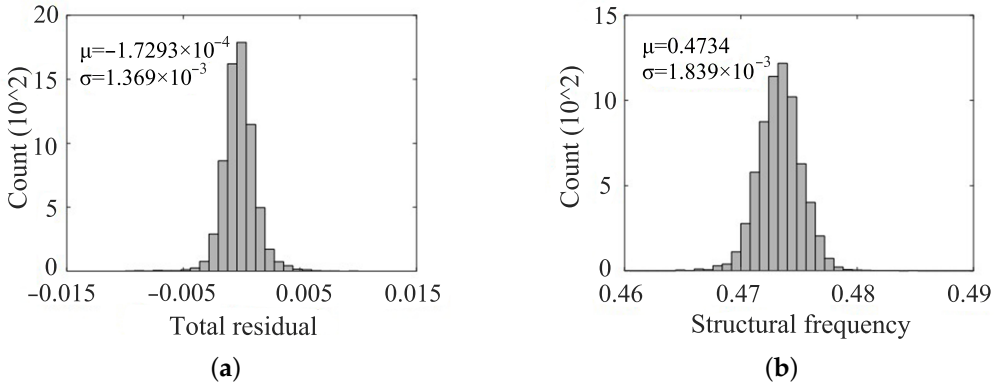

Figure 9. Comparison before and after establishing Lasso regression model: (**a**) total residual, (**b**) original structural frequency.

6. Abnormal Pattern Detection: Case Study

Due to this bridge undergoing pavement replacement work in March 2020, with half of the bridge deck still open to traffic during the replacement process, this paper will use the data collected during this period as abnormal patterns of the bridge structure to validate the proposed abnormality detection method and its effectiveness. When using the 3σ criterion as the upper- and lower-limit values for the normal state of the structure, the results of the recognition of the abnormal event of bridge deck pavement replacement using the previous Lasso regression model are as shown in Figure 10.

As can be seen from Figure 10, both the daily- and annual-scale Lasso regression models can identify the abnormal patterns of the structure. However, the Lasso regression model under the annual scale has a smaller dispersion of regression residuals, indicating that the Lasso regression model on the annual scale is more sensitive to overall changes in the bridge structure and can more effectively identify abnormal patterns.

In conclusion, this paper suggests that, in practical engineering applications, a Lasso regression model on an annual scale should be established to identify abnormal patterns of the structure by utilizing the SHM data.

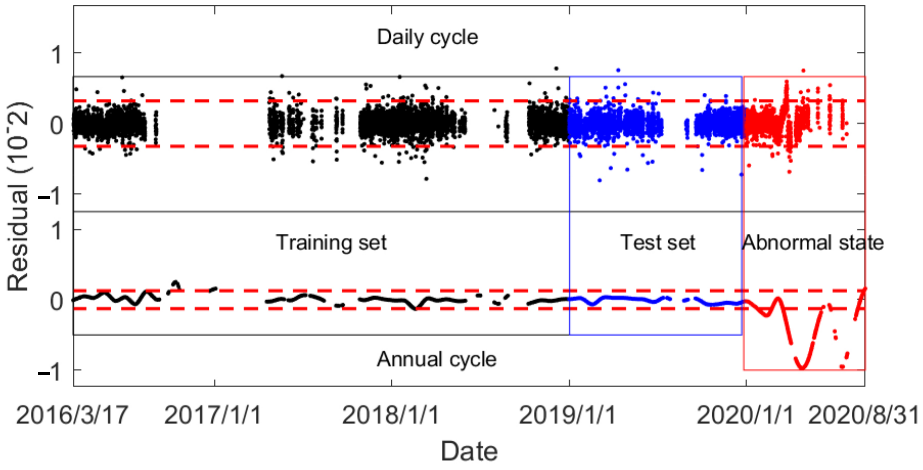

Figure 10. Structural abnormal pattern recognition results.

7. Conclusions

Based on SHM data, this paper analyzes the time-varying characteristics and correlations between structural temperature, equivalent traffic load, and structural vertical frequency. Lasso regression models under different time scales for identifying abnormal patterns are established and verified using a large-span arch bridge. The conclusions obtained were as follows:

1. For this bridge, the equivalent traffic load can be replaced by the RMS of the structural acceleration;
2. The temperature of the steel bridge structure changes uniformly, without any noticeable temperature lag in different structural components. There is a good linear relationship between the longitudinal displacement of the girder and the structure temperature, which can serve as an important basis for evaluating the performance of expansion joints;
3. It is feasible to eliminate the normal time-varying components of the structural characteristics by establishing a relationship between the action and structural characteristics;
4. The power spectral densities of structural temperature, equivalent traffic load, and structural vertical frequency exhibit two different periodic components, 24 h and 8192 h, corresponding to the daily and annual cycle scales, respectively;
5. Lasso regression models established based on frequency residuals under both daily and annual cycle scales can all identify structural abnormal states, but the predictive performance of the Lasso regression model under the annual cycle scale is better.

A further future research proposal is to consider the influence of pile–soil interaction on the structural frequency and extract indicators that are more sensitive to the structural state. Furthermore, it is necessary to study whether damage indicators established based on structural frequency are applicable to small- and medium-span bridges.

Author Contributions: Conceptualization, H.Z. and N.H.; methodology, H.Z.; software, H.H.; validation, H.Z., H.H. and Z.F.; formal analysis, H.Z.; investigation, N.H.; resources, H.H.; data curation, Z.F.; writing—original draft preparation, H.Z.; writing—review and editing, H.Z.; visualization, Z.F.; supervision, N.H.; project administration, N.H.; funding acquisition, N.H. All authors have read and agreed to the published version of the manuscript.

Funding: This research was funded by Zhejiang Engineering Center of Road and Bridge Intelligent Operation and Maintenance Technology, grant number 202302G.

Institutional Review Board Statement: Not applicable.

Informed Consent Statement: Not applicable.

Data Availability Statement: The data presented in this study are available on request from the corresponding author. The data are not publicly available due to privacy reasons.

Conflicts of Interest: The authors declare no conflicts of interest. The funders had no role in the design of the study; in the collection, analyses, or interpretation of data; in the writing of the manuscript; or in the decision to publish the results.

References

1. Ko, J.; Ni, Y. Technology developments in structural health monitoring of large-scale bridges. *Eng. Struct.* **2005**, *27*, 1715–1725. [CrossRef]
2. Wong, K. Design of a structural health monitoring system for long-span bridges. *Struct. Infrastruct. Eng.* **2007**, *3*, 169–185. [CrossRef]
3. Sun, L.; Shang, Z.; Xia, Y.; Nagarajaiah, S. Review of bridge structural health monitoring aided by big data and artificial intelligence: From condition assessment to damage detection. *J. Struct. Eng.* **2020**, *146*, 04020073. [CrossRef]
4. Shang, Z.; Sun, L.; Xia, Y.; Zhang, W. Vibration-based damage detection for bridges by deep convolutional denoising autoencoder. *Struct. Health Monit.* **2021**, *20*, 1880–1903. [CrossRef]
5. Bao, Y.; Tang, Z.; Li, H.; Zhang, Y. Computer vision and deep learning-based data anomaly detection method for structural health monitoring. *Struct. Health Monit.* **2019**, *18*, 401–421. [CrossRef]
6. Xu, Y. Making good use of structural health monitoring systems of long-span cable-supported bridges. *J. Civ. Struct. Health Monit.* **2018**, *5*, 477–1497. [CrossRef]
7. Doebling, S.; Farrar, C.; Prime, M. A summary review of vibration-based damage identification methods. *Shock Vib. Digest* **1998**, *30*, 91–105. [CrossRef]
8. An, Y.; Chatzi, E.; Sim, S.; Laflamme, S.; Blachowski, B.; Qu, J. Recent progress and future trends on damage identification methods for bridge structures. *Struct. Control Health Monit.* **2019**, *26*, e2416. [CrossRef]
9. Abdeljaber, O.; Avci, O.; Kiranyaz, S.; Gabbouj, M.; Inman, D. Real-time vibration-based structural damage detection using one-dimensional convolutional neural networks. *J. Sound Vibr.* **2017**, *388*, 154–170. [CrossRef]
10. Amiri, G.; Darvishan, E. Damage detection of moment frames using ensemble Empirical Mode Decomposition and clustering techniques. *KSCE J. Civ. Eng.* **2015**, *19*, 1302–1311. [CrossRef]
11. Necati Catbas, F.; Emin Aktan, A. Condition and damage assessment: Issues and some promising indices. *J. Struct. Eng.* **2002**, *128*, 1026–1036. [CrossRef]
12. Mao, J.; Wang, H.; Spencer, B.F. Toward data anomaly detection for automated structural health monitoring: Exploiting generative adversarial nets and autoencoders. *Struct. Health Monit.* **2021**, *20*, 1609–1626. [CrossRef]
13. Li, S.; Wei, S.; Bao, Y.; Li, H. Condition assessment of cables by pattern recognition of vehicle-induced cable tension ratio. *Eng. Struct.* **2018**, *155*, 1–15. [CrossRef]
14. Yang, Y.; Li, S.; Nagarajaiah, S.; Li, H.; Zhou, P. Real-time output-only identification of time-varying cable tension from accelerations via complexity pursuit. *Struct. Health Monit.* **2016**, *142*, 04015083. [CrossRef]
15. Tian, Y.; Xu, Y.; Zhang, D.; Li, H. Relationship modeling between vehicle-induced girder vertical deflection and cable tension by bilstm using field monitoring data of a cable-stayed bridge. *Struct. Control Health Monit.* **2021**, *28*, e2667. [CrossRef]
16. Ni, Y.; Hua, X.; Wong, K.; Ko, J. Assessment of bridge expansion joints using long-term displacement and temperature measurement. *J. Perform. Constr. Fac.* **2007**, *21*, 143–151. [CrossRef]
17. Ding, Y.; Li, A. Temperature-induced variations of measured modal frequencies of steel box girder for a long-span suspension bridge. *Int. J. Steel Struct.* **2011**, *11*, 145–155. [CrossRef]
18. Kullaa, J. Distinguishing between sensor fault, structural damage, and environmental or operational effects in structural health monitoring. *Mech. Syst. Sig. Process.* **2011**, *25*, 2976–2989. [CrossRef]
19. Chen, M.; Mao, S.; Liu, Y. Big data: A survey. *Mob. Netw. Appl.* **2014**, *19*, 171–209. [CrossRef]
20. Huang, J.; Yuan, S.; Li, D.; Li, H. A kernel canonical correlation analysis approach for removing environmental and operational variations for structural damage identification. *J. Sound Vibr.* **2023**, *548*, 117516. [CrossRef]
21. Wang, X.; Li, L.; Beck, J.; Xia, Y. Sparse bayesian factor analysis for structural damage detection under unknown environmental conditions. *Mech. Syst. Sig. Process.* **2021**, *154*, 107563. [CrossRef]
22. Zhou, Y.; Sun, L. Effects of environmental and operational actions on the modal frequency variations of a sea-crossing bridge: A periodicity perspective. *Struct. Health Monit.* **2019**, *131*, 505–523. [CrossRef]
23. Lu, S.; Yan, L.; He, X.; Guo, H. Identification of modal parameters of long-span bridges under various wind velocities. *Adv. Bridge Eng.* **2022**, *26*, 1–21. [CrossRef]
24. Hou, R.; Wang, X.; Xia, Q.; Xia, Y. Sparse Bayesian learning for structural damage detection under varying temperature conditions. *Mech. Syst. Signal Process.* **2020**, *145*, 106965. [CrossRef]

25. Xie, D.; Lu, Z.; Li, G.; Liu, J.; Wang, L. Efficient Laplace prior-based sparse Bayesian learning for structural damage identification and uncertainty quantification. *Mech. Syst. Signal Process.* **2023**, *188*, 110000. [CrossRef]
26. Oh, B.; Lee, S.; Park, H. Damage localization method for building structures based on the interrelation of dynamic displacement measurements using convolutional neural network. *Struct. Control Health Monit.* **2020**, *27*, e2430. [CrossRef]
27. Ren, C.; Aoues, Y.; Lemosse, D.; De Cursi, E. Ensemble of surrogates combining Kriging and Artificial Neural Networks for reliability analysis with local goodness measurement. *Struct. Saf.* **2022**, *96*, 102186. [CrossRef]
28. Ranstam, J.; Cool, J. LASSO regression. *Br. J. Surg.* **2018**, *105*, 1348. [CrossRef]
29. Reid, S.; Tibshirani, R.; Friedman, J. A study of error variance estimation in lasso regression. *Stat. Sin.* **2016**, *26*, 35–67. [CrossRef]
30. Hosseini, R.; Rashidi, M.; Bulaji, B.; Arani, K. Multi-objective optimization of three different SMA-LRBs for seismic protection of a benchmark highway bridge against real and synthetic ground motions. *Appl. Sci.* **2020**, *10*, 4076. [CrossRef]

Disclaimer/Publisher's Note: The statements, opinions and data contained in all publications are solely those of the individual author(s) and contributor(s) and not of MDPI and/or the editor(s). MDPI and/or the editor(s) disclaim responsibility for any injury to people or property resulting from any ideas, methods, instructions or products referred to in the content.